

Radiative Corrections to Electron-Proton Scattering*

ALLAN S. KRASS

Department of Physics, Institute of Theoretical Physics, Stanford University, Stanford, California

(Received October 30, 1961)

The radiative corrections to electron-proton scattering are calculated for an experiment in which the recoil proton is detected instead of the scattered electron. The emission of very hard photons by the scattered electrons is taken into account in the phase-space integration. This calculation is intended for high-energy experiments (up to 5 Bev) but is applicable whenever the momentum resolution of the spectrometer is small, i.e., $(\Delta P_4/P_4 \lesssim 0.1)$. Mesonic contributions to the two-photon exchange diagrams are neglected.

IN a recent paper¹ Tsai has calculated the radiative corrections to electron-proton scattering for electron beam energies up to 5 Bev. In that calculation it was assumed that the scattered electron was detected and the recoil proton left undetected.

However, when one attempts to observe electrons scattered at very large angles (i.e., near 180°) the counting rate per unit solid angle becomes small, and often the physical limitations of the accelerator and spectrometer prevent observation of electrons scattered backwards.

These difficulties have been overcome in some recent experiments^{2,3} by observing the recoil proton instead of the scattered electron. This provides much higher counting rates per unit solid angle and allows the experimenter to study even 180° electron scattering by observing protons in the forward direction.

In this paper we will calculate the radiative corrections to e - p scattering assuming that the recoil proton is detected. The results will be different from those of Tsai because the phase space available to the final state is different.

This paper will be divided as follows: part I is a discussion of the experimental conditions, part II the calculation of the elastic correction, part III the calculation

of the inelastic corrections, and part IV some numerical results and discussion.

The present work is intended as an addition to the work done by Tsai in T. The notation, metric, etc. are identical, and, wherever possible, repetition of statements made in T has been avoided.

I. EXPERIMENTAL CONDITIONS

We assume an experiment in which an electron beam strikes a stationary proton target. The recoil protons are analyzed in a spectrometer as shown in Fig. 1. The slit S_1 determines the angular resolution ($\Delta\Omega_4$) and S_2 determines the momentum resolution.

A typical momentum spectrum² obtained in this way is shown in Fig. 2. The most important features of this spectrum are its near symmetry about the peak and the fact that $\Delta P_4 \ll P_4^{\text{el}}$ (note $P_4 = |\mathbf{p}_4|$). The symmetry about the peak indicates that there is no long radiative tail to the spectrum (as there is for an electron spectrum), and that, by cutting off the data at $P_4^{\text{el}} - \Delta P_4$, one is including essentially all of the events associated with this peak.

Besides the radiative correction there are three other effects which cause the spectrum to spread:

1. finite energy spread in incident beam ($\Delta E_1/E_1 \lesssim 1\%$);
2. finite magnet aperture $\Delta\Omega_4$;
3. bremsstrahlung and straggling in target.

Effects 1 and 2 can be quantitatively calculated from elementary kinematics. The width induced in the proton spectrum by each effect is given by:

$$1. \quad \left(\frac{\Delta P_4}{P_4} \right)_{\theta'=\text{const}} = - \frac{E_4}{E_1 + M} \left(\frac{\Delta E_1}{E_1} \right). \quad (1.1)$$

$$2. \quad \left(\frac{\Delta P_4}{P_4} \right)_{E_1=\text{const}} = - \left(\frac{E_4}{M} \tan \theta' \right) \Delta \theta'. \quad (1.2)$$

In practice the error introduced into the value of the cross section by these two effects is negligible. However, if the proton is observed at angles far from the forward direction Eq. (1.2) may become important.

We assume that the effects of bremsstrahlung and straggling on the radiative correction are small, so that the former can be calculated independently, and, in our calculation, we may assume an infinitely thin target.

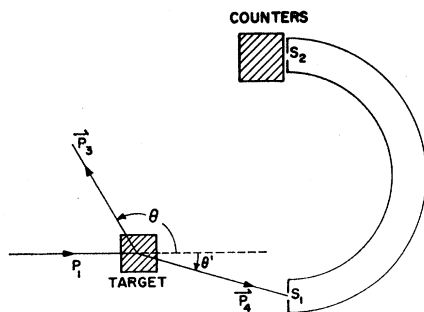


FIG. 1. Experiment arrangement for observing recoil proton.

* Supported in part by the U. S. Air Force through the Air Force Office of Scientific Research.

¹ Y. S. Tsai, Phys. Rev. **122**, 1898 (1960). Hereafter referred to as T.

² P. Gram and R. Hofstadter (private communication).

³ For example, Berkelman, Cassels, Olson, and Wilson, in *Proceedings of the 1960 Annual International Conference on High-Energy Physics at Rochester*, edited by E. C. G. Sudarshan (Interscience Publishers, New York, 1960).

II. ELASTIC CORRECTION

This correction is worked out in detail by Tsai¹, and since the final state consists of only two particles there is no essential change in the calculation when the proton is detected instead of the electron. The energy-momentum δ function ensures that a determination of p_3 fixes p_4 , and vice versa.

The only change required is the switching of the phase-space integration from the final proton momentum (case 1) to the final electron momentum (case 2).

We evaluate

$$A = \int \frac{d^3 p_3}{E_3} \frac{d^4 p_4}{E_4} \delta^4(p_1 + p_2 - p_3 - p_4) |M|^2 \quad (2.1)$$

for the two cases:

$$(\text{case 1}) \quad A_3 = (E_1/M\eta^2) d\Omega_3 |M|^2, \quad \eta = E_1/E_3^{\text{el}}, \quad (2.2)$$

$$(\text{case 2}) \quad A_4 = \frac{P_4(E_4+M)}{M(E_1+M)} d\Omega_4 |M|^2, \quad (2.3)$$

where $P_4 = (E_4^2 - M^2)^{1/2}$.

For the same incident energy and momentum transfer (q^2), the ratio of the differential elastic cross section of case 1 to that of case 2 is

$$A_3/A_4 = E_1(E_1+M)/\eta^2 P_4(E_4+M). \quad (2.4)$$

All of the comments made in T concerning the separation of the infrared parts of the elastic diagrams⁴ and the deletion of mesonic contributions^{5,6} to the two-photon diagrams are applicable in the present case as well.

The elastic correction can then be written as follows [cf. Eq. (II.13) of T]:

$$\begin{aligned} \left(\frac{d\sigma}{d\Omega_4} \right)_{\text{el}} = & \left(\frac{d\sigma}{d\Omega_4} \right)_{\text{Ros}} \left\{ 1 + \frac{\alpha}{\pi} \left[-K(p_1 p_3) + K(p_1 p_1) \right. \right. \\ & - ZK(p_2 p_1) - ZK(p_4 p_3) + ZK(p_2 p_3) \\ & + ZK(p_4 p_1) - Z^2 K(p_2 p_4) + Z^2(p_2 p_2)] \\ & + \frac{\alpha}{\pi} \left[-\frac{28}{9} + \frac{13}{6} \ln(-q^2/m^2) \right. \\ & \left. \left. + Z\pi^2 [\sin(\theta/2) - \sin^2(\theta/2)] \right] \right\} \\ & \times [\cos^2(\theta/2)]^{-1} \}. \quad (2.5) \end{aligned}$$

⁴ D. R. Yennie, S. C. Frautschi, and H. Suura, Ann. Phys. **13**, 379 (1961).

⁵ S. D. Drell and S. Fubini, Phys. Rev. **113**, 741 (1959).

⁶ N. R. Werthamer and M. A. Ruderman, Phys. Rev. **123**, 1005 (1961).

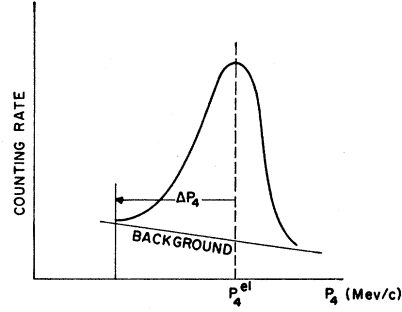


FIG. 2. Typical proton spectrum taken on Stanford linear accelerator. $P_4^{\text{el}} \approx 800$ Mev/c, $\Delta P_4 \approx 10$ Mev/c.

The Rosenbluth cross section⁷ for our case is given by

$$\begin{aligned} \left(\frac{d\sigma}{d\Omega_4} \right)_{\text{Ros}} = & \frac{r_0^2 m^2 Z^2 [\eta P_4(E_4+M)] \cos^2(\theta/2)}{4E_1^2 [E_1(E_1+M)] \sin^4(\theta/2)} \left\{ F_1^2 - \frac{q^2}{4M^2} \right. \\ & \left. \times [2(F_1 + \kappa F_2)^2 \tan^2(\theta/2) + \kappa^2 F_2^2] \right\}, \quad (2.6) \end{aligned}$$

and we define

$$\begin{aligned} \delta_{\text{el}} = & \frac{\alpha}{\pi} \left\{ -\frac{28}{9} + \frac{13}{6} \ln(-q^2/m^2) \right. \\ & \left. + Z\pi^2 [\sin(\theta/2) - \sin^2(\theta/2)] [\cos^2(\theta/2)]^{-1} \right\}. \quad (2.7) \end{aligned}$$

The angle θ is still the electron "elastic" scattering angle. The expression is simpler in this form and θ is easily obtained from θ' as follows:

$$\sin \theta = (P_4/E_3^{\text{el}}) \sin \theta'. \quad (2.8)$$

The last term of our elastic correction is the McKinley-Feshbach term.⁸ This is a second-order Born approximation for an electron scattering from a central Coulomb potential and is intended as an estimate of the non-infrared part of the two-photon exchange diagrams. The K 's are infrared terms and are defined in T.

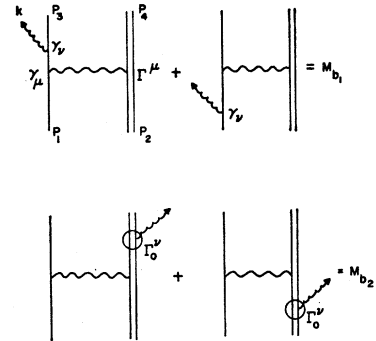


FIG. 3. Feynman graphs for the lowest order inelastic e - p scattering.

⁷ M. N. Rosenbluth, Phys. Rev. **79**, 615 (1950).

⁸ W. A. McKinley and H. Feshbach, Phys. Rev. **74**, 1959 (1948).

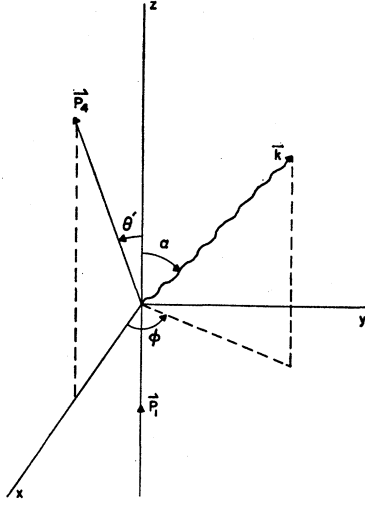


FIG. 4. Kinematics for the calculation of $\omega_{\max}(\alpha, \varphi)$.

IIIa. INELASTIC CORRECTIONS

The inelastic correction consists of the diagrams of Fig. 3. The matrix elements are given by:

$$M_{b_1} = \frac{e^3}{(2\pi)^{7/2}} \frac{mMZ}{(2\omega E_1 E_2 E_3 E_4)^{1/2}} \times \bar{u}(p_3) \left[e \frac{p_3 + k + m}{2p_3 \cdot k} \gamma_\mu - \gamma_\mu \frac{p_1 - k + m}{2p_1 \cdot k} \right] u(p_1) \times \frac{\bar{u}(p_4) \Gamma^\mu u(p_2)}{(p_1 - p_3 - k)^2}, \quad (3.1)$$

$$M_{b_2} = \frac{e^3}{(2\pi)^{7/2}} \frac{mMZ}{(2\omega E_1 E_2 E_3 E_4)^{1/2}} \frac{\bar{u}(p_3) \gamma_\mu u(p_1)}{(p_1 - p_2)^2} \times \bar{u}(p_4) \left[\Gamma_0^\nu e_\nu \frac{p_4 + k + M}{2p_4 \cdot k} \Gamma^\mu - \Gamma^\mu \frac{p_2 - k + M}{2p_2 \cdot k} \Gamma_0^\nu e_\nu \right] u(p_2), \quad (3.2)$$

$$\Gamma^\mu = F_1(q^2) \gamma^\mu + (i\kappa/M) F_2(q^2) \sigma^{\mu\nu} q_\nu, \quad (3.3a)$$

$$\Gamma_0^\mu = \gamma^\mu + (i\kappa/M) \sigma^{\mu\nu} k_\nu. \quad (3.3b)$$

(See discussion at end of IIIa.) The cross section is given by:

$$d\sigma_{\text{incl}} = \frac{(2\pi)^2 E_1 E_2}{[(p_1 \cdot p_2)^2 - m^2 M^2]^{1/2}} \times \int d^3 p_3 d^3 p_4 d^3 k \delta^4(p_1 + p_2 - p_3 - p_4 - k) \times \frac{1}{4} \sum_{\text{spins, pol.}} (M_{b_1}^\dagger + M_{b_2}^\dagger)(M_{b_1} + M_{b_2}). \quad (3.4)$$

Our problem is to perform this final-state integration for the case in which the proton is detected. In T the experimental conditions were such that the energy of an emitted photon had to be less than a value ΔE [given by Eq. (III.3) of T] in order for the event to be counted. This situation permitted a "soft photon" approximation.

However, when the proton is detected, the scattered electron can emit a very hard photon along its direction of motion without appreciably affecting the energy and direction of the recoil proton. (The analogous radiation of a hard photon in the direction of the recoil proton in case 1 is inhibited by the mass of the proton and the kinematic demands of the detectors.)

Now for a given recoil proton momentum we can calculate the distribution of photons in energy and angle using the requirements of energy-momentum conservation and the properties of the detectors. Figure 4 shows the kinematics and defines the angles we use in the calculation.⁹ Let

$$p_4 = p_4^{\text{el}} - \Delta p_4, \quad (3.5)$$

and use energy-momentum conservation to write:

$$(p_3^{\text{el}})^2 = (p_1 + p_2 - p_4^{\text{el}})^2 = m^2, \quad (3.6)$$

$$(p_3)^2 = (p_1 + p_2 - p_4 - k)^2 = m^2. \quad (3.7)$$

Subtracting (3.6) from (3.7), we derive the energy vs angle function for the emitted photons:

$$\omega_{\max}(\alpha, \varphi, \Delta P_4) = \frac{\Delta P_4}{P_4^{\text{el}} E_4^{\text{el}} E_3^{\text{el}} (1 - \cos \tau) + \Delta P_4 (\beta_4 - \cos \alpha \cos \theta' - \sin \alpha \sin \theta' \cos \varphi)} \frac{M(E_4 - M)(E_1 + M)}{P_4 E_4 E_3^{\text{el}} \Delta P_4}. \quad (3.8)$$

Here τ is the angle between p_3^{el} and k (see Fig. 5) and $\beta_4 = P_4^{\text{el}}/E_4^{\text{el}}$.

When $\Delta p_4 \ll E_3^{\text{el}}(1 - \cos \tau)$ this has the form of an ellipsoid with $\omega = 0$ at one focus. In the region ($\cos \tau \approx 1$) where ΔP_4 becomes important we can make the approximations $\cos \varphi \approx -1$ and $\alpha = \theta - \tau$. Then, since ΔP_4 is unimportant for large τ , we can use as the equation for the ellipsoid,

$$\omega_{\max}(\tau) = l(1 - \epsilon \cos \tau)^{-1}, \quad (3.9)$$

where

$$l = [M(E_4 - M)(E_1 + M)/P_4 E_4 E_3^{\text{el}}] \Delta P_4, \quad (3.10)$$

$$\epsilon = 1 - (\Delta E_4/E_3^{\text{el}}) + (\Delta P_4/E_3^{\text{el}}) \cos(\theta + \theta'). \quad (3.11)$$

This ellipsoid is very nearly cylindrically symmetric about p_3^{el} . It represents the boundary of the phase space

⁹ This calculation is very similar to that of Appendix A of T, and only the outline is presented here.

into which photons can be emitted for a maximum proton momentum loss of ΔP_4 . We now must integrate the squared matrix element formed from Eqs. (3.1) and (3.2) over this volume.

The integration is considerably simplified by breaking it into two parts.¹⁰ We first integrate over an isotropic distribution of soft photons with maximum energy ΔE [cf. Eq. (3.12)]. This includes the infrared divergences which cancel those of Eq. (2.5) and give a result similar to that obtained in T and of the same form as the well known Schwinger correction.¹¹

In the remainder of the ellipsoid the photons are assumed to be hard and nearly parallel to \mathbf{p}_3^{el} [cf. Eq. (3.18)]. For this part it is necessary to examine carefully the matrix element to find which terms become important when hard photons are emitted.

Before calculating the inelastic corrections, we must examine the effect on the form of the proton current [Eqs. (3.3a,b)] of the emission of a hard photon. Referring to Fig. 3 we see that the proton becomes virtual with the emission of a real photon. In theory these diagrams are too complex to be described in terms of only the two form factors F_1 and F_2 . For an exact treatment one would have to examine them with respect to their gauge invariance properties and obtain a more general form for the proton current containing more form factors. This corresponds to the extra probe into the structure of the proton.

In practice we keep only the form factors F_1 and F_2 , because the error we make in doing so amounts to a small correction to an already small correction. This is true, because the error is introduced by diagrams in which the hard photon is emitted by the proton current. But such an event is highly improbable, unless the proton is very relativistic (i.e., $E_4 \approx 10$ BeV). We have therefore used Eqs. (3.3a,b) to describe the two vertices at which the proton interacts with photons. We assume the usual Rosenbluth form at the virtual photon vertex and, under the assumption that the free photon does not

probe the proton deeply, the form (3.3b) at the free-photon vertex.

IIIb. SOFT PHOTONS

We take for the region of integration a small sphere of radius ΔE where ΔE is the maximum allowable photon energy in the direction \mathbf{p}_1 [see Eq. (3.8)]:

$$\Delta E = [E_1(E_1 + M)/P_4 E_4] \Delta P_4 = (1/\rho) \Delta E_4, \quad (3.12)$$

$$\rho = (P_4)^2/E_1(E_1 + M).$$

We have used the fact that most photons are emitted along the directions \mathbf{p}_1 , \mathbf{p}_3^{el} to determine ΔE . The soft-photon integration takes care of energies up to ΔE along \mathbf{p}_3^{el} , and the hard-photon integration will include the rest.

Inside the sphere ω is very small compared to all energies in the experiment so that the only important term in the matrix element is χ^2 [see Eqs. (3.22, 3.23)]:

$$\chi = \left(\frac{\mathbf{p}_3 \cdot \mathbf{e}}{\mathbf{p}_3 \cdot \mathbf{k}} - \frac{\mathbf{p}_1 \cdot \mathbf{e}}{\mathbf{p}_1 \cdot \mathbf{k}} - \frac{Z \mathbf{p}_4 \cdot \mathbf{e}}{\mathbf{p}_4 \cdot \mathbf{k}} + \frac{Z \mathbf{p}_2 \cdot \mathbf{e}}{\mathbf{p}_2 \cdot \mathbf{k}} \right).$$

The soft-photon inelastic cross section can then be written as

$$d\sigma_{\text{soft}} = \delta_{\text{soft}} d\sigma_{\text{Rosen}}, \quad (3.13)$$

wher

$$\delta_{\text{soft}} = \frac{\alpha}{4\pi^2} \int_S \frac{d^3 k}{\omega} [\sum_{\text{pol}} \chi^2]. \quad (3.14)$$

In our metric the sum over polarizations introduces a minus sign and this becomes

$$\delta_{\text{soft}} = -\frac{\alpha}{4\pi^2} \int_0^{\Delta E} \frac{k^2 dk}{\omega} \times \int d\Omega_k \left[\frac{\mathbf{p}_3}{\mathbf{p}_3 \cdot \mathbf{k}} - \frac{\mathbf{p}_1}{\mathbf{p}_1 \cdot \mathbf{k}} - \frac{Z \mathbf{p}_4}{\mathbf{p}_4 \cdot \mathbf{k}} + \frac{Z \mathbf{p}_2}{\mathbf{p}_2 \cdot \mathbf{k}} \right]^2. \quad (3.15)$$

This integration is straightforward, and the techniques are clearly outlined in T and by Yennie *et al.* in their treatment of the infrared divergences.⁴ It is sufficient then to quote the result:

$$\begin{aligned} \delta_{\text{soft}} = & -\frac{\alpha}{\pi} \left\{ \ln \frac{E_1 E_3}{(\Delta E)^2} \left[\ln \left(\frac{-q^2}{m^2} \right) - 1 + 2Z \ln \eta \right] + Z^2 \ln \frac{M E_4}{(\Delta E)^2} \left[\frac{1}{\beta_4} \ln \left(\frac{1}{\xi} \right) - 1 \right] \right\} \\ & + \frac{Z\alpha}{\pi} \left[\Phi \left(\frac{E_1 - M}{E_1} \right) - \Phi \left(-\frac{E_1 - M}{E_1} \right) + \Phi \left(\frac{2(M - E_1)}{M} \right) - \ln \frac{2E_1}{M} \ln \frac{M}{|2E_1 - M|} \right] + \frac{\alpha}{\pi} \left[\Phi \left(\frac{E_1 - E_3}{E_1} \right) + \Phi \left(-\frac{E_1 - E_3}{E_3} \right) \right] \\ & - \frac{Z\alpha}{\pi} \left[\Phi \left(-\frac{E_4 - E_1}{E_1} \right) - \Phi \left(\frac{M(E_4 - E_1)}{2E_3 E_4 - E_1 M} \right) + \Phi \left(\frac{2E_3(E_4 - E_1)}{2E_3 E_4 - E_1 M} \right) - \ln \frac{2E_3}{M} \ln \frac{2E_3 E_4 - E_1 M}{E_1 |2E_3 - M|} \right] \\ & - \frac{Z\alpha}{\pi} \left[\Phi \left(\frac{E_3 - M}{E_3} \right) - \Phi \left(-\frac{E_3 - M}{E_3} \right) + \Phi \left(\frac{2(M - E_3)}{M} \right) - \ln \frac{2E_3}{M} \ln \frac{M}{|2E_3 - M|} \right] \\ & + \frac{Z^2 \alpha}{\pi} \left[\Phi \left(\frac{\xi - 1}{\xi(\xi + 1)} \right) - \Phi \left(\frac{\xi(1 - \xi)}{\xi + 1} \right) - \Phi \left(\frac{\xi - 1}{\xi + 1} \right) + \Phi \left(-\frac{\xi - 1}{\xi + 1} \right) - \ln \frac{1}{\xi} \ln \frac{M + E_4}{2E_4} \right] \\ & + \frac{Z\alpha}{\pi} \left[\Phi \left(-\frac{E_4 - E_3}{E_3} \right) - \Phi \left(\frac{M(E_4 - E_3)}{2E_1 E_4 - E_3 M} \right) + \Phi \left(\frac{2E_1(E_4 - E_3)}{2E_1 E_4 - E_3 M} \right) - \ln \frac{2E_1}{M} \ln \frac{2E_1 E_4 - E_3 M}{E_3 |2E_1 - M|} \right]. \quad (3.16) \end{aligned}$$

¹⁰ This technique has been used by Tsai in his calculation of corrections to $e-e$ scattering: Y. S. Tsai, Phys. Rev. **120**, 269 (1960).

¹¹ J. Schwinger, Phys. Rev. **76**, 760 (1949), Eq. (2.105).

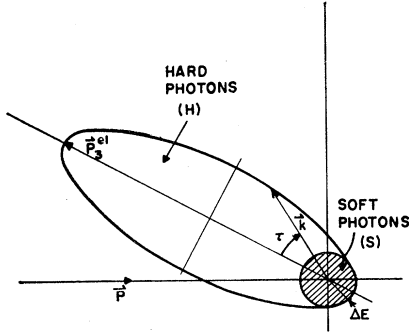


FIG. 5. Phase space available to emitted photons. The figure is an ellipsoid of revolution about \mathbf{P}_3^{el} with one focus at the origin.

Note that the infrared terms have been cancelled against those of δ_{el} . Here $\Phi(x)$ is the Spence function,¹²

$$\Phi(x) = -\int_0^x \frac{\ln|1-y|}{y} dy, \quad (3.17)$$

and

$$\xi = [(1-\beta_4)/(1+\beta_4)]^{1/2}.$$

The most important parts of δ_{soft} are the first two terms and the first term is very similar to the familiar inelastic corrections.^{1,11}

IIIc. HARD PHOTONS

Almost all the photons with energy greater than ΔE are emitted very close to the direction of \mathbf{p}_3^{el} . We take account of this fact by setting

$$k = (\omega/E_3^{el}) \mathbf{p}_3^{el}, \quad (3.18)$$

wherever k appears in scalar products with p_1, p_2, p_4 . We also notice that since $k^2=0$, we have

$$\begin{aligned} p_3 \cdot k &= (p_3^{el} + \Delta p_4 - k) \cdot k \\ &= p_3^{el} \cdot k + \Delta p_4 \cdot k \\ &\approx E_3^{el} \omega [1 - \epsilon \cos \tau], \end{aligned}$$

where

$$p_3^{el} \cdot k = E_3^{el} \omega (1 - \beta_3 \cos \tau).$$

As in Eq. (3.13), we write

$$\delta_{hard} d\sigma_{Ros} = d\sigma_{hard},$$

and a straightforward analysis yields

$$\delta_{hard} = \frac{E_3^{el} \alpha}{4\pi^2} \int_H \frac{d^3 k}{\omega E_3} \left[\frac{\frac{1}{4} \sum |M_{b_1'} + M_{b_2'}|^2}{R_0} \right], \quad (3.19)$$

where

$$E_3 = E_3^{el} + \Delta E_4 - \omega, \quad (3.20)$$

and

$$R_0 = \frac{1}{q^4} \sum_{\text{spins}} |\bar{u}(p_3^{el}) \gamma_\mu u(p_1) \bar{u}(p_4^{el}) \Gamma^\mu u(p_2)|^2.$$

R_0 is the Rosenbluth matrix element with the usual numerical factors stripped away. $M_{b_1'}$ and $M_{b_2'}$ are

defined by

$$M_{b_{1,2}} = \frac{e^3 m M Z}{(2\pi)^{7/2} (2\omega E_1 E_2 E_3 E_4)^{1/2}} M_{b_{1,2}}', \quad (3.21)$$

If the quantity

$$\frac{1}{4} \sum_{\text{spins}} |M_{b_1'} + M_{b_2'}|^2$$

is now written out, the various terms can be classified with respect to their dependence on ω . Using (3.3b) we simplify the expressions (3.1) and (3.2) and obtain:

$$M_{b_1'} = \left\{ \left[\frac{p_3 \cdot e}{p_3 \cdot k} - \frac{p_1 \cdot e}{p_1 \cdot k} \right] \frac{(\gamma_\mu)_{31} (\Gamma^\mu)_{42}}{(q)^2} + \left[\frac{ek \gamma_\mu}{2p_3 \cdot k} + \frac{\gamma_\mu ke}{2p_1 \cdot k} \right]_{31} \frac{(\Gamma^\mu)_{42}}{q^2} \right\}, \quad (3.22)$$

$$\begin{aligned} M_{b_2'} = -Z \left\{ \left[\frac{p_4 \cdot e}{p_4 \cdot k} - \frac{p_2 \cdot e}{p_2 \cdot k} \right] \frac{(\gamma_\mu)_{31} (\Gamma^\mu)_{42}}{(q+k)^2} + \frac{(\gamma_\mu)_{31}}{(q+k)^2} \right. \\ \times \left[\frac{ek \Gamma^\mu}{2p_4 \cdot k} + \frac{\Gamma^\mu ke}{2p_2 \cdot k} \right]_{42} + \frac{\kappa}{2M} \frac{(\gamma_\mu)_{31}}{(q+k)^2} \\ \left. \times \left[\frac{p_4 + M}{2p_4 \cdot k} \Gamma^\mu + \Gamma^\mu \frac{p_2 + M}{2p_2 \cdot k} \right]_{42} \right\}, \quad (3.23) \end{aligned}$$

where the expression $(\gamma_\mu)_{31} (\Gamma^\mu)_{42}$ is shorthand for $[\bar{u}(p_3) \gamma_\mu u(p_1) \bar{u}(p_4) \Gamma^\mu u(p_2)]$.

Using the approximation (3.18), we can simplify $(q+k)^2$ as follows:

$$\begin{aligned} (q+k)^2 &= q^2 + 2q \cdot k \\ &\approx (E_3/E_3^{el}) q^2. \end{aligned}$$

[E_3 defined by Eq. (3.20).] With this simplification the quantity

$$\frac{1}{4} \sum_{\text{spins}} |M_{b_1'} + M_{b_2'}|^2$$

can be written out and with the help of (3.18) all the ω dependence in each separate term can be isolated into a factor multiplying a more or less complicated trace of γ matrices.

We give here a schematic representation of the result in which the B 's represent sums of traces. It is not necessary to specify them precisely since, as we shall show, no terms involving complicated traces are important in the final result.

$$\begin{aligned} \frac{1}{4} \sum_{\text{spins}} |M_{b_1'} + M_{b_2'}|^2 &= -\frac{m^2}{(p_3 \cdot k)^2} R_0 + \frac{1}{p_3 \cdot k} \left(\frac{2E_3^2}{\omega E_3^{el}} + \frac{\omega}{E_3^{el}} + \frac{2E_3}{E_3^{el}} \right) R_0 \\ &\quad + Z^2 Q \frac{(E_3^{el})^3}{E_3 \omega^2} R_0 + \frac{4Z(\eta-1/\eta)}{q^2} \left(\frac{E_3^{el}}{\omega} \right)^2 R_0 \quad (3.24) \\ &\quad + \frac{E_3}{E_3^{el}} B_1 + \frac{E_3^{el}}{\omega} B_2 + \frac{E_3^{el}}{E_3} B_3 + B_4, \end{aligned}$$

$$Q = [q^2/(ME_1 E_3^{el})^2] [E_1 E_3^{el} + \frac{1}{4} q^2] = -\sin^2 \theta / M^2.$$

¹² K. Mitchell, Phil. Mag. 40, 351 (1949).

This now has to be integrated over the hard-photon region [Eq. (3.19)] which is the ellipsoid of Fig. 5. From Eqs. (3.9), (3.10), (3.11), and (3.12) we can write

$$l = r\Delta E, \\ \epsilon = 1 - r\Delta E/E_3^{\text{el}},$$

where

$$r = M(E_1 - E_3^{\text{el}})/E_1 E_3^{\text{el}}. \quad (3.24a)$$

Then (3.19) becomes (with $\mu = \cos\tau$):

$$\delta_{\text{hard}} = +\frac{\alpha}{2\pi} \int_{-1}^1 d\mu \int_{\Delta E}^{l/(1-\epsilon\mu)} d\omega \frac{\omega E_3^{\text{el}}}{E_3} \\ \times \left[\left(\frac{1}{4} \sum_{\text{spins}} |M_{b_1'} + M_{b_2'}|^2 \right) / R_0 \right]. \quad (3.25)$$

We may now insert (3.24) into (3.25) and perform the integrations. In all cases these can, with the aid of the Spence function, be worked out completely. When this is done, it is found that the terms containing $1/p_3 \cdot k$ and R_0 give the major contributions and that the terms containing the complicated traces are smaller than these by a factor $\Delta E/E_3^{\text{el}}$.

In the Appendix we give the results of the individual integrations, and here we give the result for δ_{hard} :

$$\delta_{\text{hard}} = +\frac{\alpha}{\pi} \left\{ 2 \ln \frac{2E_3^{\text{el}}}{r\Delta E} \ln \frac{E_3^{\text{el}}}{\sqrt{2}\Delta E} + \frac{1}{2} \ln \frac{\rho}{2} \ln \frac{E_3^{\text{el}}}{r\Delta E} \right. \\ \left. + \frac{1}{2} \left(1 + \frac{\pi^2}{6} \right) + Z(E_3^{\text{el}})^2 \left(1 + \ln \frac{r}{2} \right) \right. \\ \left. \times \left[ZQ + \frac{4(\eta - \eta^{-1})}{q^2} \right] \right\}. \quad (3.26)$$

Now the total radiative correction is calculated by combining (2.7), (3.16), and (3.26):

$$\delta_{\text{total}} = \delta_{\text{el}} + \delta_{\text{soft}} + \delta_{\text{hard}},$$

and

$$\left(\frac{d\sigma}{d\Omega} \right)_{\text{total}} = \left(\frac{d\sigma}{d\Omega} \right)_{\text{Ros}} (1 + \delta_{\text{total}}). \quad (3.27)$$

IV. NUMERICAL EXAMPLES AND DISCUSSION

It is interesting to compare the radiative corrections obtained here for proton detecting experiments with that obtained in T for electron experiments. We would also like to compare our result in the limit of low-incident electron energies with that obtained by Schiff.¹³

Case 1: $E_1 = 900$ Mev, $E_3 = 327$ Mev, $\eta = 2.75$, $\Delta P_4 = 10$ Mev.

	$e^- + p$ ($Z = +1$)	$e^+ + p$ ($Z = -1$)
δ_{el}	+8.1%	+5.9%
δ_{soft}	-30.2%	-22.9%
δ_{hard}	+5.5%	+6.0%
δ_{total}	-16.6%	-11.0%

¹³ L. I. Schiff, Phys. Rev. **87**, 750 (1952).

These corrections are somewhat smaller than the corresponding ones for electron detection (see T, part IV).

Some care must be taken in comparing the results of Schiff's calculation with those obtained in this problem. Schiff's calculation was intended for an emulsion experiment in which the protons were resolved only in angle and not in energy. All protons with momenta above some small value were to be observed. Clearly this situation is inconsistent with our assumption that $\Delta P_4/P_4$ is very small (i.e., $\Delta P_4/P_4 \lesssim 0.1$).

We can get a rough comparison with Schiff's result by using $(\Delta P_4/P_4) = 0.1$ in both his formula and ours. For $\theta' = 0$ Schiff's formula in our notation becomes [cf. Eq. (7), reference 13]:

$$(\delta_{\text{total}})_{\text{Schiff}} = -\frac{\alpha}{\pi} \left\{ \left[\ln \left(\frac{2E_1}{m} \right) - \frac{1}{2} \right] \right. \\ \left. \times \left[\ln \frac{(x-1)^2}{x} + x + \frac{11}{6} \right] - \frac{17}{13} - \frac{\pi^2}{6} \right\},$$

where $x = 2E_1/q_m$ and $q_m = P_4 \min$.

Now for $E_1 = 100$ Mev, $E_3 = 82.5$ Mev, $\Delta P_4 = 18$ Mev/c,

$$\delta_{\text{total}} = -2.4\% \quad (\text{Schiff}),$$

$$\delta_{\text{total}} = -3.8\% \quad (\text{our value}).$$

This agreement is quite good and serves as a check on the validity of our approximations.

We can summarize the regions of validity of the two corrections as follows:

1. The Schiff correction is valid for a nonrelativistic final proton (i.e., $\beta_4 \ll 1$) and for $\Delta P_4 \approx P_4^{\text{el}}$.
2. Our correction is good when $\beta_4 \geq 0.3$ and $\Delta P_4/P_4 \lesssim 0.1$.

This latter restriction is quite conservative, and in high-energy experiments $\Delta P_4/P_4$ will usually be much smaller than this.

ACKNOWLEDGMENTS

The author is indebted to Professor Yung-Su Tsai for his help and encouragement in this work, and to Peter Gram and Edwin Erickson for useful discussions of experimental problems.

APPENDIX

We wish to perform the integrations indicated in Eq. (3.25) using the expression (3.24) for the matrix element. After a reduction involving the partial fraction expansions,

$$\frac{(E_3^{\text{el}})^2}{E_3^2 \omega} = \frac{2}{E_3} + \frac{\omega}{E_3^2} + \frac{1}{\omega} \quad (A.1)$$

and

$$\frac{E_3^{e1}}{E_3\omega} = \frac{1}{E_3} + \frac{1}{\omega}, \quad (A.2)$$

the integral (3.25) becomes

$$\begin{aligned} \delta_{\text{hard}} = & \frac{\alpha}{2\pi} \int_{-1}^1 d\mu \int_{\Delta E}^{l/(1-\epsilon\mu)} d\omega \left\{ -\frac{m^2}{(E_3^{e1})^2(1-\epsilon\mu)^2} \right. \\ & \times \left[\frac{1}{E_3} + \frac{1}{\omega} \right] + \frac{1}{E_3^{e1}(1-\epsilon\mu)} \left[\frac{E_3^{e1}}{E_3} + \frac{2E_3^{e1}}{\omega} - 1 \right] \\ & + \left[Z^2 Q + \frac{4Z(\eta - \eta^{-1})}{q^2} \right] \frac{(E_3^{e1})^2}{\omega} + \frac{B_1'}{E_3^{e1} R_0} \\ & \left. + \frac{E_3^{e1} B_2'}{E_3 R_0} + \frac{E_3^{e1} B_3'}{E_3^2 R_0} + \frac{B_4'}{R_0} \right\}. \quad (A.3) \end{aligned}$$

The (B') 's differ from the B 's only in the possible addition of extra terms from partial fraction expansions. If the integrals involving (B') 's are worked out, it is found that all of them are of order $\Delta E/E_3^{e1}$ compared with the terms involving R_0 . Since $\Delta E \ll E_3^{e1}$ and $B'/R_0 \approx 1$, these terms are all negligible.

The first three terms can be integrated directly, and the results are as follows:

$$E_3^{e1} \int_{-1}^1 d\mu \int_{\Delta E}^{l/(1-\epsilon\mu)} d\omega \left[-\frac{m^2}{(E_3^{e1})^2(1-\epsilon\mu)^2} \times \left(\frac{1}{E_3} + \frac{1}{\omega} \right) \right] \approx O\left(\frac{m^2}{(\Delta E)^2}\right).$$

We assume $\Delta E \gg m$ and therefore can drop this term.

$$\begin{aligned} & \int_{-1}^1 d\mu \int_{\Delta E}^{l/(1-\epsilon\mu)} d\omega \frac{1}{(1-\epsilon\mu)} \left[\frac{1}{E_3} + \frac{2}{\omega} - \frac{1}{E_3^{e1}} \right] \\ & \approx 4 \ln \frac{2E_3^{e1}}{r\Delta E} \ln \frac{E_3^{e1}}{\sqrt{2}\Delta E} + \ln \frac{\rho}{2} \ln \frac{E_3^{e1}}{r\Delta E} + \left(1 + \frac{\pi^2}{6} \right), \quad (A.4) \end{aligned}$$

where ρ and r are given by (3.12) and (3.24a).

$$E_3^{e1} \int_{-1}^1 d\mu \int_{\Delta E}^{l/(1-\epsilon\mu)} d\omega \left(\frac{E_3^{e1}}{\omega} \right) = 2(E_3^{e1})^2 \left(1 + \ln \frac{r}{2} \right). \quad (A.5)$$

We have consistently neglected Spence functions $\Phi(x)$ in which $|x| \ll 1$. When $x \ll -1$ we can approximate $\Phi(x)$ by

$$\Phi(x) \approx -\frac{\pi^2}{6} - \frac{1}{2} [\ln x]^2 \quad (x \ll -1). \quad (A.6)$$

This equation has been used in (A.4). Now Eqs. (A.4) and (A.5) are inserted into (A.3) to give (3.26).